Catal Lett (2009) 128:127–136
DOI 10.1007/s10562-008-9703-2

Nickel Oxide Based Supported Catalysts for the In-situ Reactions of Methanation and Desulfurization in the Removal of Sour Gases from Simulated Natural Gas

**Wan Azelee Wan Abu Bakar · Mohd Yusuf Othman ·
Rusmidah Ali · Ching Kuan Yong**

Received: 6 August 2008 / Accepted: 24 September 2008 / Published online: 11 November 2008
© Springer Science+Business Media, LLC 2008

Abstract Supported nickel oxide based catalysts were prepared by wetness impregnation method for the in-situ reactions of H_2S desulfurization and CO_2 methanation from ambient temperature up to 300 °C. Fe/Co/Ni (10:30:60)–Al_2O_3 and Pr/Co/Ni (5:35:60)–Al_2O_3 catalysts were revealed as the most potential catalysts, which yielded 2.9% and 6.1% of CH_4 at reaction temperature of 300 °C, respectively. From XPS, Ni_2O_3 and Fe_3O_4 were suggested as the surface active components on the Fe/Co/Ni (10:30:60)–Al_2O_3 catalyst, while Ni_2O_3 and Co_3O_4 on the Pr/Co/Ni (5:35:60)–Al_2O_3 catalyst.

Keywords Nickel oxide · Catalyst · Methanation · Desulfurization · Natural gas

1 Introduction

Malaysian crude natural gas is categorized as a sour gas due to the contamination of carbon dioxide (CO_2) and hydrogen sulfide (H_2S). Catalysts for the CO_2 methanation have been extensively studied because of their application in the conversion of CO_2 gas to produce methane, which is the major component in natural gas. In fact, there is also presence of H_2S in real natural gas. Therefore, H_2S should be considered in invention of methanation catalyst, since it could cause poisoning of the nickel catalyst. However, fewer researches on the catalyst for in-situ reactions of CO_2 methanation and desulfurization have been carried out.

The acidic nature of CO_2 and H_2S necessitates the employment of a catalytic system with basic properties such as Group VIII metals. According to Miao et al. [1], the activity and selectivity of the catalysts are most probably related to the changeable valence of M^0/M^{2+}. The major reasons for the much slower development of the catalysts science of mixed metal oxide is its significant complexity compared with metal based catalysts e.g. possible presence of multiple oxidation states, variable local coordination, coexisting bulk and surface phases as well as different surface termination functionalities such as M–OH, M $=$ O or M–O–M [2]. Nickel based catalysts are generally considered as reference methanation catalysts and proven to eliminate H_2S by desulfurization process. According to Inui et al. [3], the CO_2 methanation activity of the nickel based composite catalyst from the substrates of iron group metals following this order: Ni $>$ Co $>$ Fe. El-Shobaky et al. [4] observed a significant increment in the catalytic activity of NiO/MgO system due to treatment with small amount of CoO. Souma et al. [5] investigated that methanation reaction seems to be accelerated by the absorption of H_2 on metallic Ni or Co. Medina et al. [6] concluded that carbon dioxide hydrogenation on Fe has the advantage of no catalyst deactivation. Praseodymium has been investigated as the most effective rare earth metal oxide when it was doped onto NiO based catalysts for CO_2 methanation reaction at 400 °C. Later, cobalt oxide was found as the most suitable dopant towards the Pr/Ni catalyst (WA Wan Abu Bakar, “Personnel Communication” 2005). The addition of increasing amounts of Pr_6O_{11} caused the conversion rate of side product to decrease with an apparent minimum [7]. The selection of support is considered as important since it may influence both the activity and selectivity of the reaction. It has been

W. A. Wan Abu Bakar (✉) · M. Y. Othman · R. Ali ·
C. K. Yong
Department of Chemistry, Faculty of Science, Universiti
Teknologi Malaysia, 81310 UTM Skudai, Johor, Malaysia
e-mail: wanazelee@yahoo.com

discovered that the addition of alumina may increase the methanation activity although there is presence of low concentration of H_2S [8].

The nickel oxide based catalysts should be capable to achieve both low temperature and high conversion of sour gases to be applicable in gas industry. At low temperature, application of the novel catalyst in gas industry is more likely. However, problem arises because exothermic reaction of conversion of CO_2 to CH_4 is unfavorable at low temperature due to its low energy content.

2 Materials and Methods

2.1 Preparation of Catalysts

$Ni(NO_3)_2 \cdot 6H_2O$ was dissolved with minimum amount of distilled water. Mixed catalysts solution was prepared by mixing appropriate amount of metal nitrate salts. Wet impregnation method was used to prepare Al_2O_3 supported catalyst by impregnating the catalyst solution on Al_2O_3 beads support for 15 min. It was then dried at 80 °C for 24 h and calcined in air at 400 °C for 5 h.

2.2 Catalytic Activity Measurements

The supported catalyst sample was packed into a cylindrical glass tube with diameter of 10 mm and length of 360 mm and was stored in the furnace of the home-built micro reactor as shown in Fig. 1. No pretreatment was done prior to beginning the heating experiment. In-situ reactions of methanation and desulfurization were performed from ambient temperature up to 300 °C with the increment temperature rate of 5 °C/min. Each experiment was repeated twice and each treatment temperature was maintained for 30 min before the next temperature increment was accomplished. It was found that the catalytic activity on the second treatment did not differ significantly. Composition of the reactant gases is depicted in Table 1, in comparison with the real composition of sour gases in Malaysian crude natural gas. The mixture of CO_2 and H_2 gases were introduced into the reactor system in a stoichiometric ratio of 1:4. The product gas coming out from the furnace was collected in FTIR sample cell and scanned at every 20 °C by FTIR Shimadzu 8300 Spectrometer. Percentage conversion of CO_2 and H_2S was obtained by calculating the peak area of their respective stretching bands relative to the peak area of the gas during calibration without catalyst. Off line GC analysis (Hewlett Packard 6890 Series GC System) was done to determine the yield of CH_4 gas due to the low sensitivity of FTIR spectroscopy towards the stretching band of CH_4.

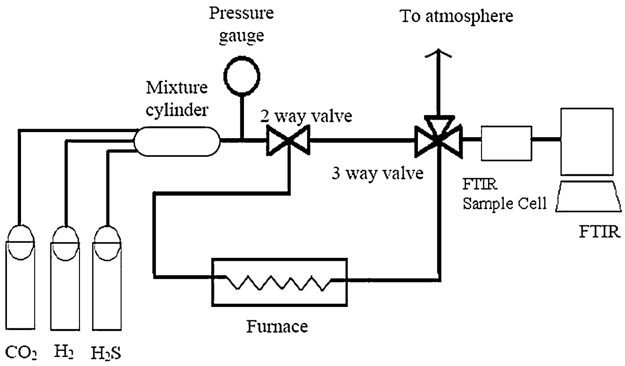

Fig. 1 Schematic diagram of home-built micro reactor

Table 1 Reaction data with closely chemical composition to crude natural gas from Telaga Bergading, Petronas Carigali Sdn. Bhd., analyzed by GC-MS[a]

Gas	Reaction data (%)	Composition in crude natural gas (%)
CH_4	–	47.9
CO_2	19.0	23.5
H_2S	4.8	5.4
Others (CO, O_2, N_2)	–	24.1
H_2	76.2	–

[a] GC-MS was conducted at UNIPEM, Universiti Teknologi Malaysia, 2003

2.3 Characterization of Catalysts

XPS analysis was done by using Kratos instrument XSAM HS surface analysis spectrometer with MgKα X-ray source (1253.6 eV). Sample was introduced into the spectrometer in flowing argon atmosphere, and evaporated at least 6×10^9 Torr before spectrum was recorded. The spectrum was taken at 10 mA and 14 kV energy source at 2 sweeps. N_2 adsorption–desorption isotherms for the catalysts were measured by Micromeritics ASAP 2010. All samples were evacuated at 120 °C prior to the measurement.

3 Results and Discussion

3.1 In-situ Reactions of Methanation and Desulfurization

Al_2O_3 supported NiO based catalyst was modified by different additives (Co, Fe, Cu, Mn, Pr, Sm, Zr) to study the effect of modification additive. Table 2 shows the overall conversion of CO_2 and H_2S resulted from screening by FTIR spectroscopy up to reaction temperature of 300 °C.

At the highest studied temperature of 300 °C, supported Co/Ni (40:60)–Al_2O_3 catalyst showed 90% conversion of

Table 2 Percentage conversion of CO_2 and H_2S resulted from catalytic screening monitored by FTIR spectroscopy

Catalyst	% Conversion of CO_2			% H_2S desulfurization		
	100 °C	200 °C	300 °C	100 °C	200 °C	300 °C
Co/Ni (40:60)	3.77	9.28	15.95	18.44	78.38	90.00
Mn/Ni (40:60)	7.57	4.47	1.33	50.60	91.31	89.98
Cu/Ni (40:60)	9.86	13.77	5.72	93.76	96.88	100.00
Pr/Ni (40:60)	10.99	11.43	11.2	43.19	86.54	100.00
Zr/Ni (40:60)	6.32	4.26	2.19	5.05	84.90	90.38
Fe/Co/Ni (5:35:60)	9.07	7.67	9.12	88.10	91.17	100.00
Fe/Co/Ni (10:30:60)	14.33	12.48	11.52	50.69	91.84	100.00
Mn/Co/Ni (5:35:60)	9.81	8.18	17.71	47.30	93.36	58.45
Mn/Co/Ni (10:30:60)	7.78	9.20	5.03	77.70	92.29	100.00
Fe/Mn/Ni (5:35:60)	9.04	10.14	16.45	53.81	93.38	95.60
Fe/Mn/Ni (10:30:60)	8.08	10.67	4.08	71.20	92.92	93.84
Fe/Mn/Co/Ni (5:10:25:60)	8.32	3.10	2.95	47.19	96.47	100.00
Pr/Co/Ni (5:35:60)	11.08	14.80	19.19	49.09	62.00	100.00
Pr/Co/Ni (10:30:60)	10.03	12.02	16.75	65.04	93.45	100.00
Pr/Cu/Ni (5:10:85)	8.83	13.84	6.76	61.02	91.87	100.00
Pr/Cu/Ni (3:7:90)	15.66	11.82	8.35	52.40	63.08	100.00
Sm/Zr/Ni (5:25:70)	7.76	8.87	13.84	82.40	90.66	100.00

H_2S and 16% conversion of CO_2. When manganese acted as a dopant (Mn/Ni (40:60)–Al_2O_3), it generally gave low catalytic activity, which did not exceed 10% conversion of CO_2. The H_2S desulfurization activity also decreased at reaction temperature higher than 280 °C. The conversion rate of CO_2 over Mn/Co/Ni (5:35:60)–Al_2O_3 catalyst was increasing from reaction temperature of 200 °C to 300 °C. However, its H_2S desulfurization activity reduced starting from 220 °C and showed a sudden drop at 300 °C. On the other hand, the CO_2 conversion activity over Mn/Co/Ni (10:30:60)–Al_2O_3 and Fe/Mn/Co/Ni (5:10:25:60)–Al_2O_3 catalysts was less than 10% throughout the catalytic testing. This phenomenon could be explained in terms of reactivity, where MnO is easy to react with SO_2 to form $MnSO_4$, an inactive compound that may deactivate the catalyst [9]. When MnO contained in a higher composition as in Fe/Mn/Ni (5:35:60 and 10:30:60)–Al_2O_3 catalysts, there is an abnormal phenomenon occurred at 70–80 °C. This is due to the adsorption property possessed by the catalysts that may inhibit the CO_2 methanation reaction. Manganese is not a good dopant for nickel based catalyst. This is in good agreement with Wachs et al. [2], which concluded that, some active basic metal oxide components such as MnO, CeO etc. do not interact strongly with the different oxide functionalities present on oxide support and consequently, do not disperse very well to form crystalline phases.

The catalytic activity of Cu/Ni (40:60)–Al_2O_3 catalyst showed the highest 13.8% conversion of CO_2 at reaction temperature of 200 °C. However, it was decreased at reaction temperature higher than 200 °C. 100% H_2S desulfurization was achieved over this catalyst at 280 °C. Pr/Ni (40:60)–Al_2O_3 catalyst generally showed unstable CO_2 conversion rate that fluctuated around $10 \pm 3\%$. It could be assumed that the adsorption property of the catalyst deteriorated its catalytic activity. However, it was able to show 100% of H_2S desulfurization at 250 °C. When praseodymium was added towards Cu/Ni catalyst, Pr/Cu/Ni (5:10:85)–Al_2O_3 catalyst did not show a higher conversion of H_2S and CO_2 compared to Cu/Ni (40:60)–Al_2O_3 catalyst. Pr/Cu/Ni (3:7:90)–Al_2O_3 catalyst with 7% loading of Cu was reported as the optimum ratio towards Ni by Tavares et al. [10], who worked on silica-supported Ni and Ni–Cu catalysts in $CO + H_2$ mixtures. However, this catalyst was deactivated slowly by time. This is presumably due to the occurrence of undesired side reactions at higher temperature. In addition, CuO is similar with MnO. It may also react with SO_2 to form inactive compounds that would deactivate the catalyst [9].

Fe/Co/Ni (10:30:60)–Al_2O_3 catalyst reached the highest 16.5% conversion of CO_2 at reaction temperature of 120 °C. The conversion rate remained above 10% although it was slightly reduced at higher reaction temperature. Similar result had also been reported where the conversion of CO_2 at 192 °C was 14% over Fe/SiO_2 catalyst [6]. Co and Fe could be assigned as good dopants towards NiO based catalyst. They are active basic metal oxides that usually anchor to the oxide substrate by preferentially titrating the surface Lewis acid sites, such as surface M-[ ] vacancies, of the oxide support [2]. This is also in agreement with Wang et al. [9] that CO_2 was strongly chemisorbed on the Fe (110) surface with the strongest binding energy. However, Fe is unfavoured in larger amount because it tends to reduce the performance of the catalyst by oxidizing the CO intermediate back to CO_2 [11].

The conversion activities of CO_2 and H_2S over Pr/Co/Ni (5:35:60)–Al_2O_3 catalyst was lower compared to the Fe/Co/Ni (10:30:60)–Al_2O_3 catalyst at low reaction temperature. However, its catalytic performance increased drastically at reaction temperature of 300 °C. Pr is believed to be able to assist in the generation of active site for the in-situ reactions of CO_2 methanation and H_2S desulfurization at elevated temperature. Miao et al. [1] had observed that rare earth metal oxides could increase the stability of catalyst during high temperature and avoid the sintering of nickel. Yamasaki et al. [12] have been reported that amorphous alloy of Ni–25Zr–5Sm catalyzed the methanation reaction with 90% conversion of CO_2 and 100% selectivity towards CH_4 at 300 °C. However, Sm/Zr/Ni (5:25:70)–Al_2O_3 catalyst prepared by wet impregnation technique in this research did not perform such a high catalytic activity as performed by the above said amorphous alloy catalyst.

Figure 2 shows the details trend plot of the CO_2 conversion and H_2S desulfurization activities over both of the potential catalysts: Fe/Co/Ni (10:30:60)–Al_2O_3 and Pr/Co/Ni (5:35:60)–Al_2O_3 catalysts.

In this research, H_2S is converted to unharmful sulfur and water as shown in the equation below. The presence of sulphur was supported by the Energy Dispersive X-ray Analysis (EDX) that revealed 0.94% of sulfur on the spent Pr/Co/Ni (5:35:60)–Al_2O_3 catalyst, while 2.68% of sulfur on the spent Fe/Co/Ni (10:30:60)–Al_2O_3catalyst.

$$H_2S + {}^1\!/\!{}_2O_2 \rightarrow S + H_2O$$

There are two possible reactions occurred during the CO_2/H_2 methanation reaction. Carbon monoxide and water would also be formed in addition to methane. The production of methane gas was determined by GC due to the low sensitivity of FTIR spectroscopy towards the absorption band of methane. Table 3 depicts the testing results of in-situ reactions of CO_2 methanation and H_2S desulfurization by the potential Al_2O_3 supported NiO based catalysts.

CO_2 could be physisorbed on most of the metal surfaces according to Wambach and Freud [13]. Two states of molecular associative adsorption were observed for CO_2 on the clean metal surfaces: a physisorbed linear CO_2 state and a bent chemisorbed CO_2 state. The chemisorbed, partially negatively charged species turns out to be the precursor for CO_2 dissociation. It had been reported that CH_4 formation from carbon is easier on Co (100) than on Fe (110) [14]. The presence of subsurface carbon tends to increase the activation energy required for the hydrogenation steps and hence CH_4 formation becomes more difficult in the presence of Fe-carbides. Therefore, Fe/Co/Ni

Table 3 Testing results of CO_2/H_2 methanation reaction during in-situ reactions condition over Al_2O_3 supported NiO based catalysts

Catalyst	Temperature (°C)	Converted CO_2 (%)[a]		Unreacted CO_2 (%)
		CH_4	CO + H_2O	
Fe/Co/Ni (10:30:60)–Al_2O_3	100	0.50	13.83	85.67
	150	1.12	11.93	86.95
	200	1.51	10.97	87.52
	250	2.44	11.75	85.81
	300	2.89	8.63	88.48
Pr/Co/Ni (5:35:60)–Al_2O_3	100	0.41	10.67	88.92
	150	0.39	14.61	85.00
	200	0.66	14.14	85.20
	250	1.81	13.53	84.66
	300	6.09	13.10	80.81

[a] Calculation based on CO_2 detected via FTIR and CH_4 detected via GC

Fig. 2 Conversion plot of CO_2 conversion and H_2S desulfurization over potential Al_2O_3 supported Fe/Co/Ni (10:30:60) and Pr/Co/Ni (5:35:60) catalysts

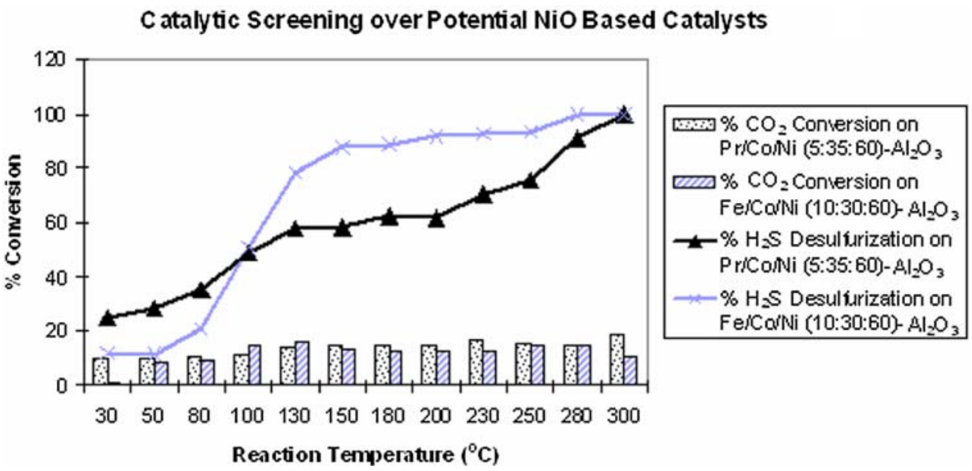

(10:30:60)–Al_2O_3 catalyst could not achieve high methanation reaction at higher studied temperature compared to Pr/Co/Ni (5:35:60)–Al_2O_3 catalyst.

Generally, methane selectivity over the supported catalyst is higher as the CO_2 conversion is increased. Davis [15] found out the major reason for the increment of methane formation when there is high CO conversion, is due to the presence of higher concentration of water. The selectivity towards CH_4 over the potential supported catalysts in this research was low, especially at ambient temperature. Most of the converted CO_2 did not yield CH_4 but tend to form CO. This is due to the indirect conversion of CO_2 into C_1 hydrocarbons, via the intermediate formation of CO, as suggested by Silver [16]. Furthermore, carbon dioxide readily forms bicarbonate. This bicarbonate may decompose to CO and CO_2. Therefore, the conversion of CO_2 in this research could be considered as incomplete as it yielded higher percentage of CO, which is the intermediate, before yielding CH_4, which is the final desired product.

3.2 Characterization of Catalysts

3.2.1 X-ray Photoelectron Spectroscopy (XPS)

Figure 3 shows the XPS spectra resulted from wide scan in the region of 0–1,100 eV, while Fig. 4 reveals high resolution XPS spectra obtained over fresh and spent Pr/Co/Ni (5:35:60)–Al_2O_3 catalysts. Table 4 depicts the parameters obtained by deconvolution of XPS spectra for these two catalysts.

1.57% of Ni was detected in the surface composition of fresh Pr/Co/Ni (5:35:60)–Al_2O_3 catalyst. The binding energies of Ni (2*p*) were characteristic of NiO at the E_b of 854.21 eV ($2p_{3/2}$) and 871.72 eV ($2p_{1/2}$). Similar assignment of NiO to the data obtained also made by Lorenz et al. [17] who studied XPS on NiO/SiO_2 and NiO–Al_2O_3/SiO_2 catalysts; and Nefedov et al. [18] who investigated on oxides of various elements. E_b value of 529.41 eV resulted from the deconvolution of O (1 *s*) also confirmed the existence of NiO. However, the existence of Ni (2*p*) peak at E_b of 856.83 eV ($2p_{3/2}$) and 874.30 eV ($2p_{1/2}$) was attributed to the existence of Ni^{3+} in Ni_2O_3. According to Nascente [19] who worked on Ni/Pd thin metallic film, E_b of 856 eV was corresponding to Ni_2O_3. Alumina supported nickel oxide calcined at 350 °C also revealed the characteristic peak corresponding to Ni^{3+} at $E_b = 856.9$ eV [20]. The most intense peak at E_b of 531.52 eV resulted from deconvolution of O (1 *s*) over the fresh catalyst also referred to the existence of Ni_2O_3 and Al_2O_3. Ni^{3+} showing a higher binding energy because the E_b of the metal increases when the covalency decreases [21]. In other words, as the ionic radius of $Ni^{2+} > Ni^{3+}$ and furthermore the covalency of Ni^{3+} decreases compare to Ni^{2+}. Ni^{3+} is known to be more reactive than Ni^{2+} due to its higher metallic property. Ni_2O_3 is suggested to be responsible as active site for this catalyst. By observing $2p_{3/2}$ peak area, the existence of NiO was observed as 31% more than Ni_2O_3. When NiO was more dominant on the fresh Pr/Co/Ni (5:35:60)–Al_2O_3 catalyst, low catalytic activity was observed. It is presumed that the lower H_2S desulfurization

Fig. 3 XPS spectra resulted from wide scan of fresh and spent Pr/Co/Ni (5:35:60)–Al_2O_3 catalysts

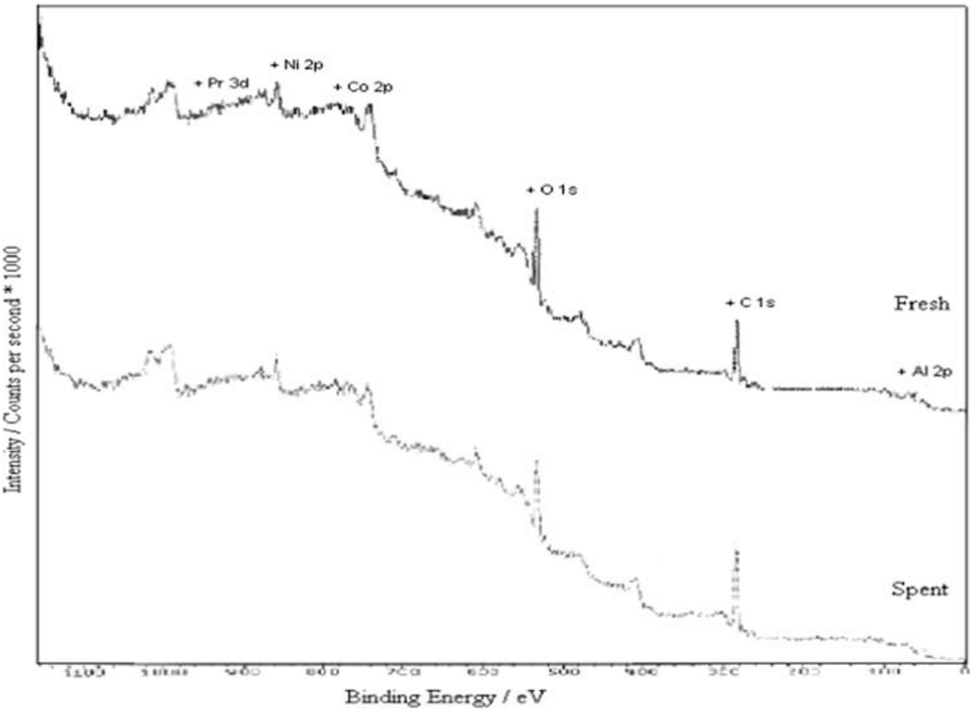

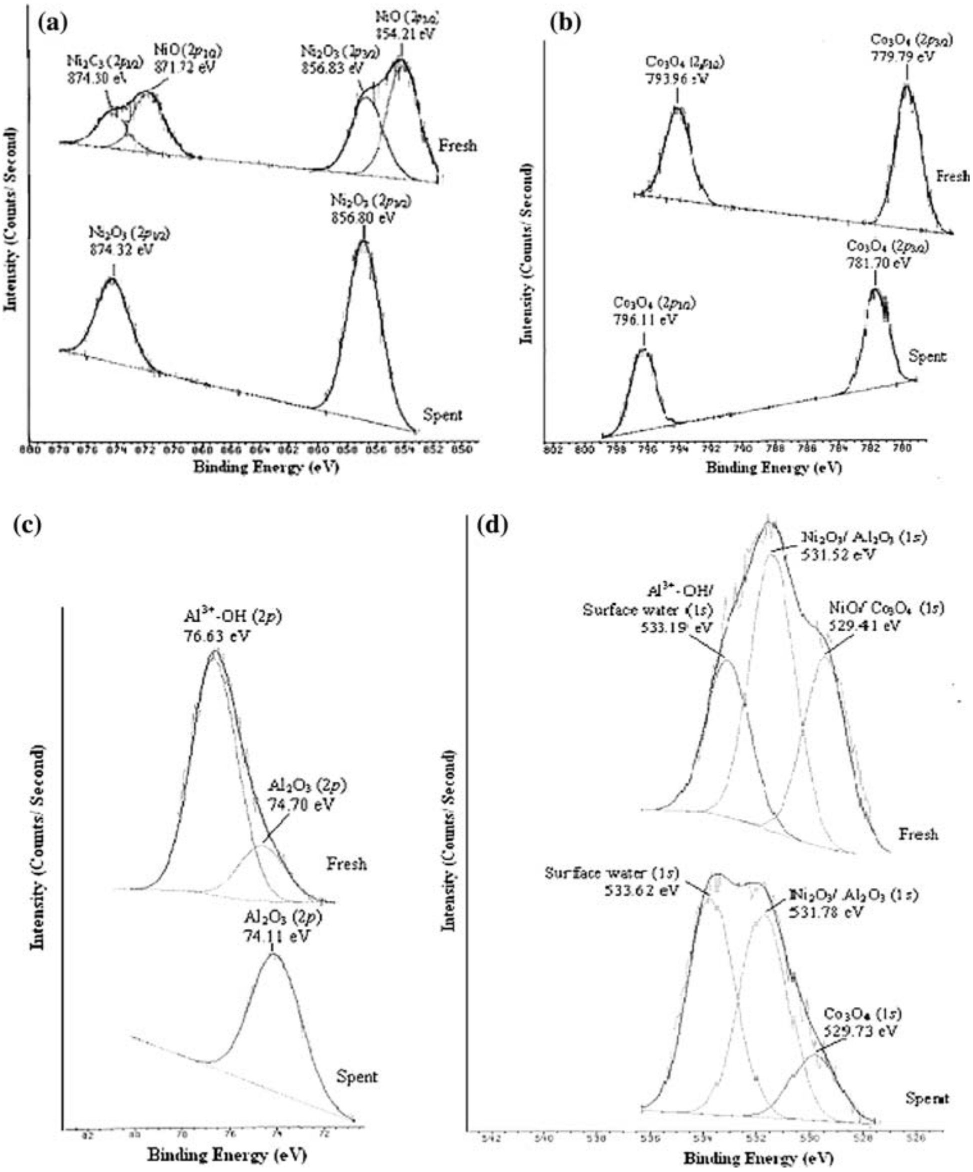

Fig. 4 High resolution **a** Ni 2*p*, **b** Co 2*p*, **c** Al 2*p*, and **d** O 1 *s* XPS spectra obtained from fresh and spent Pr/Co/Ni (5:35:60)–Al_2O_3 catalysts

Table 4 Parameters obtained by deconvolution of XPS spectra for fresh and spent Pr/Co/Ni (5:35:60)–Al_2O_3 catalysts

Catalyst	Phase	Ni $2p_{3/2}$	Ni $2p_{1/2}$	Co $2p_{3/2}$	Co $2p_{1/2}$	Al 2*p*	O 1 *s*
Pr/Co/Ni (5:35:60)–Al_2O_3 fresh	NiO	854.21	871.72				529.41
	Ni_2O_3	856.83	874.30				531.52
	Co_3O_4			779.79	793.96		529.41
	Al_2O_3					74.70	531.52
	Al^{3+}–OH					76.63	533.19
	Surface hydroxyl						533.19
Pr/Co/Ni (5:35:60)–Al_2O_3 spent	Ni_2O_3	856.80	874.32				531.78
	Co_3O_4			781.70	796.11		529.73
	Al_2O_3					74.11	531.78
	Surface hydroxyl						533.62

activity over Pr/Co/Ni (5:35:60)–Al_2O_3 catalyst at reaction temperature below 200 °C was due to lack of Ni_2O_3, which is an oxygen rich compound. Ni_2O_3 structure is believed to play an important role in the nickel cation reduction and the oxygen release process [22]. This suggestion is further supported when the dominant nickel form on the surface of Ni impregnated AlMCM-41 catalyst was found out to be Ni_2O_3 [23], as such contribute bigger surface area.

After exposure towards the catalytic testing environment, the surface composition of Ni^{3+} was increased to 2.28%. The existing peaks were attributed to Ni^{3+} in Ni_2O_3 species at the E_b value of 856.80 eV ($2p_{3/2}$) and 874.32 eV ($2p_{1/2}$). NiO was disappeared in the spent catalyst. This was also supported by 59% reduction of peak area on the O (1 *s*) peak at 529.73 eV. It is believed that NiO was transformed into Ni_2O_3 during prolong catalytic testing process. Similar phenomenon was also reported by Djaidja et al. [24], where NiO phase was disappeared in their used Ni/Sm_2O_3 and Ni/La_2O_3 catalysts. They suggested that Ni_2O_3 phase is necessary in the oxidative transformation of methane reaction course. Dong et al. [25] had also observed the growth of Ni_2O_3 layers on the surface of Ni particles after exposure in a mixture of H_2 and Ar gas atmosphere of 760 Torr. No NiO phase was detected by them. The absence of NiO is presumably responsible for the increasing of the catalytic performance over this catalyst at maximum study temperature of 300 °C.

There was 0.49% of Co revealed in the surface composition of fresh Pr/Co/Ni (5:35:60)–Al_2O_3 catalyst. Binding energies of 779.79 eV ($2p_{3/2}$) and 793.96 eV ($2p_{1/2}$) suggesting the presence of spinel compound, Co_3O_4, on the surface of the catalyst. This is in good agreement with Kim [26] who studied the electronic structure of cobalt oxides and Zeng et al. [27] who worked on the effect of ZrO_2 matrix on surface Co_3O_4–CO position. The presence of Co_3O_4 is supported by the O (1 *s*) peak at E_b value of 529.41 eV, which was also suggested by Natile and Glisenti [28], who studied on NiO/Co_3O_4 nanocomposite catalyst. NO_2 formed during the decomposition of $Co(NO_3)_2 \cdot 6H_2O$ in the preparation could oxidize Co^{2+} to Co^{3+} even at low calcination temperature. The Co ions have a high tendency to form Co_3O_4 once oxidized [29]. The existence of the spinel compound in the catalyst is presumed to be good for the catalytic efficiency as it provides more active sites for the reaction and also it could change forms easily according to the environment; whether it is more to Co^{2+} or Co^{3+}. After catalytic testing, the Co (2*p*) peaks shifted to a higher E_b of 781.70 eV ($2p_{3/2}$) and 796.11 eV ($2p_{1/2}$), but indicating no changes of Co oxidation state on the surface of the catalyst. The O (1 *s*) peak remained in the same region, at E_b of 529.73 eV, with 59% reduction of peak area. This peak is attributed to the existence of Co_3O_4 only. This reduction on peak area was due to the disappearance of NiO. 0.48% of Co was still observed on the spent catalyst surface. In this stage, an optimum amount of Co spinel compound is presumed to be the reason for the increasing of the catalytic activity [30].

There are two Al (2*p*) peaks obtained from the fresh Pr/Co/Ni (5:35:60)–Al_2O_3 catalyst, indicating the existence of Al in two different environments. At E_b value of 74.70 eV, it is attributed to Al_2O_3. The O (1 *s*) peak at 531.52 eV also referred to the existence of Al_2O_3. When Al atom is on the outermost surface, the influence of the surrounding chemical environment on Al 2*p* spectrum is significant. On the outer surface, alumina is in contact with atmosphere and absorbed water. Therefore, the surrounding chemical environment of alumina on the outer surface is different from that in inner layer [31]. This contributed to the formation of Al^{3+}–OH which was shown at E_b of 76.63 eV. As the binding energy increases, so does the ionic character of the bonding. Wojcieszak et al. [23] also observed similar XPS result from their AlMCM-41 support. Al_2O_3 (E_b 75 eV) was assigned to framework aluminium species and to extra framework Al^{3+} ($E_b = 77.5$ eV). The extra framework Al^{3+} species is easily affected by the surrounding environment. Adsorbed water on the catalyst surface or Al^{3+} with the surface hydroxyl was observed at the O (1 *s*) E_b value of 533.19 eV. However, only one peak was detected at E_b value of 74.11 eV on the spent catalyst. It is attributed to the existence of Al_2O_3. The detected weight percentage of Al also decreased in the spent catalyst compared to the fresh catalyst; in agreement with the only peak existed in the spent catalyst. After exposure to the catalytic testing environment, the increment of O (1 *s*) peak area at 533.62 eV is due to the adsorbed water on the surface, one of the products from methanation reaction.

From the surface composition detected by XPS, 0.09% of Pr was revealed on the surface of fresh Pr/Co/Ni (5:35:60)–Al_2O_3 catalyst. After catalytic activity measurement, the percentage of Pr was reduced to 0.02%. This reduction would be either due to the deposition of sulfur, or agglomeration of other elements that forced the Pr element to move into the bulk of the catalyst.

Figure 5 depicts XPS spectra resulted from wide scan in the region of 0–1,100 eV. The high resolution XPS spectra over fresh Fe/Co/Ni (10:30:60)–Al_2O_3 catalyst is shown in Fig. 6.

The atomic concentration of Ni detectable by XPS was low (0.93%), indicating the possibility of partial surface encapsulation of Ni in the alumina support [20]. The Ni ($2p_{3/2}$) and Ni ($2p_{1/2}$) peaks at $E_b = 856.67$ eV and 874.37 eV are registered in the XPS spectra of Ni 2*p* level of the fresh Fe/Co/Ni (10:30:60)–Al_2O_3 sample, respectively. This assignment is also been suggested by Nascente [19] and Salagre [20]. The O 1 *s* peak at E_b of 531.77 eV obtained from fresh Fe/Co/Ni (10:30:60)–Al_2O_3 catalyst

Fig. 5 XPS spectra resulted from wide scan of fresh Fe/Co/Ni (10:30:60)–Al_2O_3 catalyst

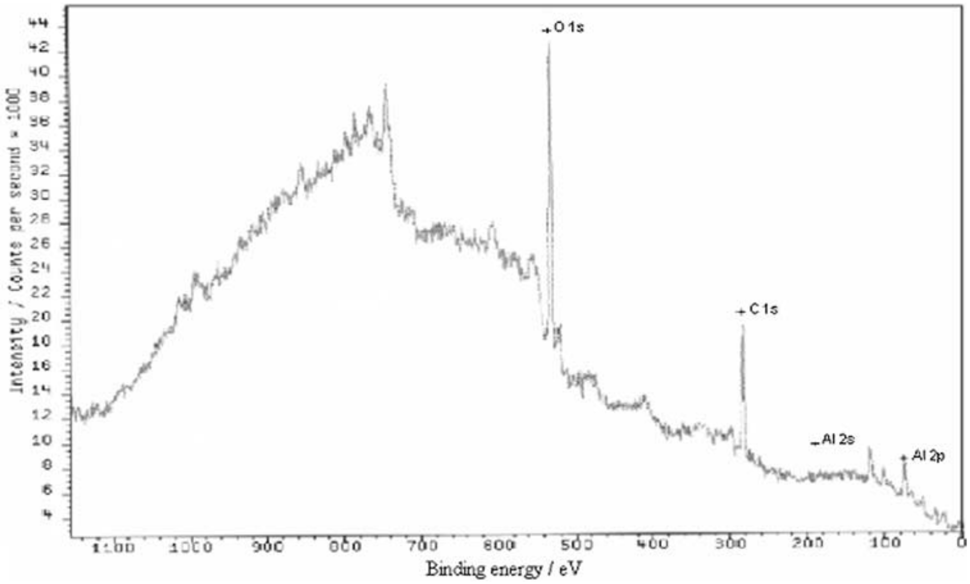

Fig. 6 High resolution **a** Ni 2*p*, **b** Fe 2*p*, **c** Al 2*p*, and **d** O 1 *s* XPS spectra obtained from fresh Fe/Co/Ni (10:30:60)–Al_2O_3 catalyst

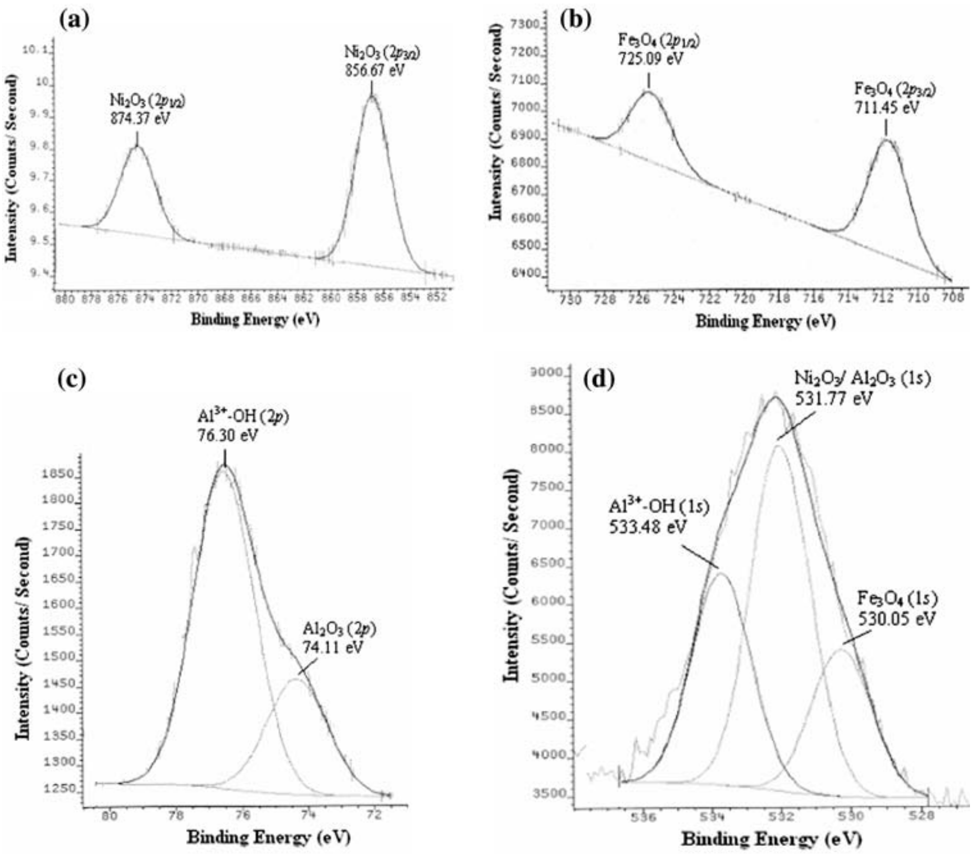

was attributed to the O^{2-} in Ni_2O_3. Ni_2O_3 could act as an active site for oxidation reaction because its oxygen storage property is needed for the H_2S desulfurization reaction. It is known that the presence of Ni^{3+} may enhance the p-type character (oxygen rich) of the catalyst.

0.66% of Fe was revealed in the surface composition. The oxides of α-Fe_2O_3, γ-Fe_2O_3 and Fe_3O_4 have almost identical core binding energies, but the absence of satellite peak had confirmed that the E_b at 711.45 eV ($2p_{3/2}$) and 725.09 eV ($2p_{1/2}$) is due to Fe_3O_4. This is also supported by the appearance of O 1 *s* peak at E_b of 530.05 eV. This assignment is in good agreement with McIntyre and Zetaruk [32], who studied iron oxides with XPS and Yamashita and Hayes [33], who had analyzed XPS spectra of Fe^{2+} and Fe^{3+} ions in oxide materials. It is believed that spinel compound of Fe_3O_4 is good for the catalytic reaction as it able to provide more active sites. Based on the mechanism of the Fischer-Tropsch synthesis involving unreduced iron catalyst [34], it is attractive to consider the oxidized state of iron as the active phase in Fischer-Tropsch synthesis. It is of interest to note that the partially pre-reduced catalyst containing Fe_3O_4 as a major phase was more active than the catalyst pre-reduced to α-Fe^{2+}. According to Iyer et al. [35], Fe_3O_4 was also reported as active phase in their enhanced hydrogen production integrated with CO_2 separation.

There are two peaks indicating Al^{3+} in Al_2O_3 ($E_b = 74.11$ eV) and Al^{3+}–OH ($E_b = 76.30$ eV) on the fresh Fe/Co/Ni (10:30:60)–Al_2O_3 catalyst. When Al is on the outermost surface, it is in contact with atmosphere and absorbed water thus resulting in higher E_b.

Merely 0.08% of cobalt was revealed in the surface composition compared to 0.66% of iron. Similar condition was also detected by Kozhukharov et al. [36], where the Co 2*p* partial contribution was not well expressed when there was presence of iron. It is believed that Co ions react with the substrates during the calcination and sintering process. Part of them being high chemical mobility and reactivity are incorporated into the bulk of the support. Furthermore, previous study suggested that the sorption affinity of cations depends not only on the valence of the cations but also on their radius. The ionic radii of Co^{2+} and Co^{3+} are 74 pm and 61 pm while Fe^{2+} and Fe^{3+} are 78 and 65 [37]. The smaller radii of the Co ions could disperse highly into the matrix and penetrate deeper into the support. Therefore, results in lower surface concentration of Co. The synthesis of highly dispersed Co catalysts requires the initial formation of very small CoO or Co_3O_4 crystallites. The formation of these small oxide clusters in turn requires strong interactions between the support and the Co precursor [38]. Because the mean free path of electrons in solids is very small, the detected electrons originate from only the top few atomic layers. While ionization occurs to a depth of a few micrometers, only those electrons that originate within tens of angstroms below the solid surface can leave the surface without energy loss [39].

3.2.2 Nitrogen Adsorption Analysis

From Table 5, the surface area of the spent Pr/Co/Ni (5:35:60)–Al_2O_3 catalyst is 8.6% higher than the surface area of its fresh catalyst. As such for this catalyst, it can be concluded that the increment of the surface area, did increase the catalytic activity of the Pr/Co/Ni (5:35:60)–Al_2O_3 catalyst at higher temperature (300 °C). By referring to the XPS analysis, it was known that Co ions with high mobility were incorporated into the bulk of the support when there was presence of Fe ions. For the Pr/Co/Ni (5:35:60)–Al_2O_3 catalyst, Co ions were detected as spinel compound of Co_3O_4 on the surface. Therefore, Co_3O_4 is presumed to give contribution on the increment of surface area over this catalyst. Besides that, NiO was present in the fresh Pr/Co/Ni (5:35:60)–Al_2O_3 catalyst but disappeared after catalytic testing. The transformation of NiO into Ni_2O_3 is believed to be able to generate new active sites for the in-situ reactions of methanation and desulfurization. In addition, the Ni_2O_3 phase was suggested to serve as a matrix to decrease the Ni atom agglomeration [23]. Consequently, the surface area is increased when there is generation of new active sites. The average pore diameter of Pr/Co/Ni (5:35:60)–Al_2O_3 catalyst was increased after catalytic testing. The enlargement of pore diameter over the spent catalyst is believed to be resulted by the collapsed of pores during the prolonged testing condition.

Table 5 BET surface area and BJH desorption average pore diameter of the Fe/Co/Ni (10:30:60)–Al_2O_3 and Pr/Co/Ni (5:35:60)–Al_2O_3 catalysts in fresh and spent conditions

Catalyst	Condition	S_{BET} ($m^2\ g^{-1}$)	d (nm)
Fe/Co/Ni (10:30:60)–Al_2O_3	Fresh	175.01	9.24
Fe/Co/Ni (10:30:60)–Al_2O_3	Spent	165.37	5.12
Pr/Co/Ni (5:35:60)–Al_2O_3	Fresh	166.22	5.63
Pr/Co/Ni (5:35:60)–Al_2O_3	Spent	180.45	5.88

On the other hand, there was 5.5% reduction on the BET surface area of spent Fe/Co/Ni (10:30:60)–Al_2O_3 catalyst. This reduction is believed to result from the deposition of sulfur (from EDX analysis; not shown) on the catalyst surface or collapsed of the pores. The smaller pore diameter shown by spent catalyst also proved the blockage of the pores by sulfur. Catalytic activity over this catalyst also decreased after reaching maximum 16.5% conversion of CO_2 at 120 °C. The BET surface area is reduced when there is no generation of new active sites. No transformation of active species occurred during the catalytic reaction as reported by XPS analysis.

4 Conclusion

According to XPS analysis, Ni_2O_3 and Co_3O_4 were suggested as the active sites on the Pr/Co/Ni (5:35:60)–Al_2O_3 catalyst. Meanwhile, Ni_2O_3 and Fe_3O_4 acted as the active phases on the Fe/Co/Ni (10:30:60)–Al_2O_3 catalyst. The aim to achieve high H_2S desulfurization rate at low temperature was achieved. However, further investigation is still needed in the attempt to obtain catalyst that is able to catalyze high CO_2 methanation rate at low temperature in the presence of H_2S, which is a deactivation source.

Acknowledgements The authors are gratefully acknowledged to the Ministry of Science, Technology and Innovation, Malaysia for IRPA Vot 79252 and Universiti Teknologi Malaysia for financial support.

References

1. Miao Q, Xiong G, Sheng S, Cui W, Xu L, Guo X (1997) Appl Catal A 154:17
2. Wachs IE (2005) Catal Today 100:79
3. Inui T, Funabiki M, Suehiro M, Sezume T (1979) J Chem Soc Faraday Trans 75:787
4. El-Shobaky GA, El-Molla SA, Ali AMI (2003) Appl Catal A 253:417
5. Souma Y, Ando H, Fujiwara M, Kieffer R (1995) Energy Convers Manage 36:593
6. Medina JC, Butala SJ, Bartholomew CH, Lee ML (2000) Fuel 79:89
7. Wang WD, Lin PY, Fu YL, Cao GY (2002) Catal Lett 82:19
8. Happel J, Hnatow MA (1981) Alumina-containing methanation catalysts. U.S. Patent 4,260,553
9. Wang HT, Xiao TC, Su JX, Liu WX, Lu YL (1999) Catal Today 53:661
10. Tavares MT, Alstrup I, Bernardo CA, Rostrup-Nielsen JR (1996) J Catal 158:402
11. Medina JC, Butala SJ, Bartholomew CH, Lee ML (2000) Geochim Cosmochim Acta 64:643
12. Yamasaki M, Komori M, Akiyama E, Habazaki H, Kawashima A, Asami K, Hashimoto K (1999) Mater Sci Eng A 267:220
13. Wambach J, Freud H (1994) In: Paul J, Pradier CM (eds) Carbon dioxide chemistry: environmental issues. The Royal Society of Chemistry, Cambridge
14. Fournier JA (1986) Characterization of some iron catalysts for the reduction of carbon monoxide and the effect of residence time and temperature on the nature of carbon monoxide reduction products. PhD Thesis. Brown University, United States of America
15. Davis BH (2007) Ind Eng Chem Res 46:8938
16. Silver RG, Jackson NB, Ekerdt JG (1988) In: Ayers WT (ed) Catalytic activation of carbon dioxide. American Chemical Society Washington, DC
17. Lorenz P, Finster J, Wendt G, Salyn JV, Žumadilov EK, Nefedov VI (1979) J Electron Spectrosc Relat Phenom 16:267
18. Nefedov VI, Gati D, Dzhurinskii BF, Sergushin NP, Salyn YaV, Russ J (1975) Inorg Chem 20:2307
19. Nascente PAP (2005) J Mol Catal A 228:145
20. Salagre P, Fierro JLG, Medina F, Sueiras JE (1996) J Mol Catal A 106:125
21. Vederine JC, Hollinger G, Minh OT (1978) J Phys Chem 82:1515
22. Yoon WS, Hanson J, McBreen J, Yang XQ (2006) Electrochem Commun 8:859
23. Wojcieszak R, Monteverdi S, Mercy M, Nowak I, Ziolek M, Bettahar MM (2004) Appl Catal A 268:241
24. Djaidja A, Barama A, Bettahar MM (2000) Catal Today 61:303
25. Dong XL, Zhang ZD, Jin SR, Sun WM, Chuang YC (1998) Nanostr Mater 10:585
26. Kim KS (1975) Phys Rev B 11:2177
27. Zeng HC, Lin J, Tau KL (1995) J Mater Res 10:3096
28. Natile MM, Glisenti A (2003) Chem Mater 15:2502
29. Arnoldy P, Moulijn JA (1985) J Catal 93:38
30. Zhang YQ, Jacobs G, Sparks DE, Dry ME, Davis BH (2002) Catal Today 71:411
31. Zheng HY, An MZ, Lu JF (2008) Appl Surf Sci 254:1644
32. McIntyre NS, Zetaruk DG (1977) Analy Chem 49:1521
33. Yamashita T, Hayes P (2008) Appl Surf Sci 254(8):2441
34. Blanchard F, Reymond JP, Pommier B, Teichner SJ (1982) J Mol Catal 17:171
35. Iyer M, Ramkumar S, Fan LS (2006) Annual technical progress report. The Ohio-State University, United States of America
36. Kozhukharov V, Machkova M, Brashkova N (2003) J Sol Gel Sci Tech 26:753
37. Weast RC, Selby SM (1966) Handbook of chemistry and physics, 47th edn. The Chemical Rubber Co, Ohio
38. Iglesia E (1997) Appl Catal A 161:59
39. Moulder JF, Stickle WF, Sobol PE, Bomben KD (1992) Handbook of X-ray photoelectron spectroscopy. Perkin-Elmer Corporation, United States of America